Carotenoid Radical Cations as a Probe for the Molecular Mechanism of Nonphotochemical Quenching in Oxygenic Photosynthesis

ARTICLE *in* THE JOURNAL OF PHYSICAL CHEMISTRY B · MAY 2007

Impact Factor: 3.3 · DOI: 10.1021/jp066458q · Source: PubMed

6 AUTHORS, INCLUDING:

Sergiu Amarie
Neaspec GmbH
31 PUBLICATIONS **416** CITATIONS
SEE PROFILE

Jörg Standfuss
Paul Scherrer Institut
30 PUBLICATIONS **1,420** CITATIONS
SEE PROFILE

Andreas Dreuw
Universität Heidelberg
154 PUBLICATIONS **6,773** CITATIONS
SEE PROFILE

Josef Wachtveitl
Goethe-Universität Frankfurt am Main
182 PUBLICATIONS **3,751** CITATIONS
SEE PROFILE

Carotenoid Radical Cations as a Probe for the Molecular Mechanism of Nonphotochemical Quenching in Oxygenic Photosynthesis

Sergiu Amarie,[†] Jörg Standfuss,[‡] Tiago Barros,[‡] Werner Kühlbrandt,[‡] Andreas Dreuw,[†] and Josef Wachtveitl*,[†]

Institute for Physical and Theoretical Chemistry, Johann Wolfgang Goethe-University—Frankfurt, Max-von-Laue-Strasse 7, 60438 Frankfurt am Main, Germany, and Max Plank Institute of Biophysics, Department of Structural Biology, Max-von-Laue-Strasse 3, 60438 Frankfurt am Main, Germany

Received: October 2, 2006; In Final Form: February 8, 2007

Nonphotochemical quenching (NPQ) is a fundamental mechanism in photosynthesis which protects plants against excess excitation energy and is of crucial importance for their survival and fitness. Recently, carotenoid radical cation ($Car^{\bullet+}$) formation has been discovered to be a key step for the feedback deexcitation quenching mechanism (qE), a component of NPQ, of which the molecular mechanism and location is still unknown. We have generated and characterized carotenoid radical cations by means of resonant two color, two photon ionization (R2C2PI) spectroscopy. The $Car^{\bullet+}$ bands have maxima located at 830 nm (violaxanthin), 880 nm (lutein), 900 nm (zeaxanthin), and 920 nm (β-carotene). The positions of these maxima depend strongly on solution conditions, the number of conjugated C═C bonds, and molecular structure. Furthermore, R2C2PI measurements on the light-harvesting complex of photosystem II (LHC II) samples with or without zeaxanthin (Zea) reveal the violaxanthin (Vio) radical cation ($Vio^{\bullet+}$) band at 909 nm and the $Zea^{\bullet+}$ band at 983 nm. The replacement of Vio by Zea in the light-harvesting complex II (LHC II) has no influence on the Chl excitation lifetime, and by exciting the Chls lowest excited state, no additional rise and decay corresponding to the $Car^{\bullet+}$ signal observed previously during qE was detected in the spectral range investigated (800−1050 nm). On the basis of our findings, the mechanism of qE involving the simple replacement of Vio with Zea in LHC II needs to be reconsidered.

Introduction

Carotenoids in photosynthetic organisms fulfill important functions in light harvesting and photoprotection.[1,2] As light-harvesting pigments carotenoids complement the absorption spectrum by covering the blue and green spectral region not accessible by chlorophylls (Chls).[3,4] In addition, they scavenge dangerous singlet oxygen molecules and quench both singlet and triplet states of the photosynthetic apparatus.[5−9] The fundamental molecular processes underlying these functions are energy and electron transfer between carotenoids and Chls.[1,10]

Feedback deexcitation, a component of NPQ, is an important process in the photoprotection of plants by which excess excitation energy of Chls is dissipated as heat.[11] The activation of qE is linked to an increase in the pH gradient across the thylakoid membrane upon light saturation of the photosynthetic electron transport.[8,11,12] Vio is converted to Zea in the xanthophyll cycle, and PsbS, a protein subunit of photosystem II for which a central role in qE has been reported,[13] is protonated.[13,14] Although the interconversion of Vio to Zea in the xanthophyll cycle is a prerequisite for complete qE induction, the detailed molecular mechanism of qE remains elusive. Today even the exact role of carotenoids in this process is unclear and thought to be either direct,[15] indirect,[16] or both.[17]

According to the so-called "gear-shift" model,[15] Zea acts as a direct quencher of electronically excited Chls, since its first singlet excited electronic state (S_1) is supposed to be lower than the lowest excited Chl state (Q_y). Excitation energy transfer (EET) from Chl *a* to Zea is thus in principle possible and dissipation at Zea can take place.[15,18] In contrast, the S_1 state of Vio is supposed to be above the Q_y level of Chl *a* and thus cannot quench the Chl *a* excited state. This mechanism has been recently tested and indeed occurs in artificial light-harvesting dyads.[19]

An indirect role of the carotenoids is postulated in the aggregation model, suggesting the LHC II as the quenching site.[16,20] This model predicts that the conversion of Vio to Zea induces conformational changes of the proteins, by which new pigment configurations capable of quenching arise. Recently, the formation of Chl dimers as quenching sites has been suggested.[16]

A model that combines both direct and indirect roles of the carotenoids is the hypothesis that a quenching complex between Chl *a* and Zea is formed during the induction time of qE, in which Zea also acts as the terminal quencher.[21−24]

Apart from elucidating the molecular mechanism, it remains to be shown exactly where and in which pigment−protein complex of the photosynthetic apparatus qE actually occurs. Studies on the *Arabidopsis thaliana* npq4-1 mutant that lacks both qE and the protonation-induced absorption change at 535 nm suggest strongly that the PsbS protein contributes to photoprotective energy dissipation.[13] This implies that the quenching site might be PsbS, since binding of Zea to PsbS in vitro has been reported to give rise to a strong red shift in the

* To whom correspondence should be addressed. E-mail: wveitl@theochem.uni-frankfurt.de. Phone: +49 (0)69 798 29351. Fax: +49 (0)69 798 29709. Address: Max-von-Laue-Str 7, 60438 Frankfurt am Main, Germany.

† Johann Wolfgang Goethe-University—Frankfurt.

‡ Max Plank Institute of Biophysics.

10.1021/jp066458q CCC: $37.00
Published on Web 03/15/2007

absorption spectrum,[25] providing a possible explanation for the absorption change observed at 535 nm when qE is active.[26,27] Moreover, the resonance Raman spectrum of the in vitro Zea−PsbS complex has the same features as found in vivo during qE.[25,28]

However, another recent qE model proposes an indirect role of PsbS.[16] According to this model, PsbS interacts with LHC II in the photosynthetic membrane at low lumenal pH, inducing a conformational change and resultant quenching in the same way as observed in vitro upon crystallization of the antenna complex. Recently it was reported that PsbS has two different aggregation states with different affinities for the core and the LHC antenna.[29] At pH 4, the protein exists as a monomer and preferentially associates with the antenna LHCs. At pH 7, a PsbS dimer, its favored aggregation state, mainly co-migrates with the photosystem II core. Together with the observation that PsbS dimers monomerize upon qE induction in intact systems the thylakoid lumen acidifies.[29−31] This suggests that monomers associated with the LHC antenna are responsible for energy dissipation in vivo.[32]

On the other hand, an appealingly simple mechanism, based on the recently determined molecular structure of LHC II,[33,34] reconsidered LHC II as the location of qE.[34] This was based on the consideration that replacement of Vio by Zea in its binding pocket of LHC II should enable quenching via EET from Chl to Zea or via electron transfer (ET) from Zea to Chl. The latter possibility is predicted by theory and indeed it has been confirmed experimentally that carotenoid radical cations are formed during qE.[17,21,22] As a consequence, if ET and not EET is the main component of qE, the efficiency of qE depends on the ionization potential of the carotenoids and the properties of the detected carotenoid radical cations rather than on the energetic position of S_1. In general, there are few studies addressing the properties of carotenoid radical cations directly. Although β-Car$^{\bullet+}$ in RC has been studied for over 20 years,[35,36] only recently, spectroscopic investigations of such cations generated electrochemically in solution have been reported.[36,37] Carotenoid radical cations have also been observed in LH2 from purple bacteria upon direct carotenoid excitation.[38,39]

In the present work, we use multiple light pulses to investigate the ultrafast dynamics of carotenoid radical cation formation both in solutions of the pure compounds and in LHC II isolated from plant thylakoids. The three-pulse technique involves contributions from two high-intensity pulses initiating a R2C2PI process and a low-intensity broad-band probe pulse. Our R2C2PI measurements reveal the spectroscopic properties of Car$^{\bullet+}$ and the spectral characteristics of Zea and Vio radical cations in LHC II, which are crucial for understanding the qE protection mechanism in higher plants.

Materials and Methods

Sample Preparation. For the measurements in solution, Vio, Lut, Zea, and β-Car powders were dissolved in ethanol to an optical density (OD) of 1 at the red wing of the 0−0 vibronic band of the $S_0 \rightarrow S_2$ transition. The Vio, Lut, and Zea were purified from spinach by HPLC,[40] whereas β-Car was purchased from Sigma.

Thylakoid membranes from pea leaves were prepared as described.[41] By incubation of the thylakoid membranes at pH 5.3 in the presence (40 mM) or absence of ascorbate, we were able to prepare samples with or without Zea. LHC II isolation was subsequently performed as in ref 34. Pigment composition of LHC II samples was determined by high performance liquid chromatography (HPLC), by the integration of HPLC peaks measured at 440 nm.[42] Every LHC II sample was measured once. For the spectroscopic experiments, the typical sample OD was 0.8/mm at 660 nm. Sample stability was confirmed by measuring the absorption spectra before and after the time-resolved measurements.

Ultrafast Transient Absorption. The time-resolved measurements were performed using a CLARK CPA 2001 (Dexter, MI) laser/amplifier system operating at a repetition rate of ~1 kHz at a central wavelength of 775 nm.[43,44] The amplified pulses were divided into three parts: two pump pulses and one probe pulse. The first excitation pulses were generated using a noncollinear optical parametric amplifier (NOPA). The maximum excitation energy was kept at 10 nJ for 660 nm pulses and 60nJ for 490 nm pulses. For the second pulse used for the R2C2PI experiment the direct output from the amplifier with a pulse energy of 200 nJ was used. For the probe pulses a white light continuum was generated by focusing amplified 775 nm light into a 5 mm sapphire window and a RG 830 filter was used to select the useful spectral region. Femtosecond time delays between pump and probe were controlled by a delay line covering times up to 1.5 ns. The time delay between the 490 and the 775 nm pump pulses was kept constant during the measurements. To minimize accumulation of photoproducts, the sample was translated continuously both horizontally and vertically in a direction normal to the bisector of the pump and probe beams at ~10 cm/s.

Computational Methods. The equilibrium structures of the carotenoid radical cations have been optimized using density functional theory (DFT) employing the standard Becke three-parameter Lee−Yang−Parr (B3LYP)[45] functional and the standard 6-31G* basis set. At these geometries, the vertical excited states have been calculated employing time-dependent DFT[46,47] with the generalized-gradient Becke−Lee−Yang−Parr (BLYP)[48] functional and 6-31G* basis set combination. Previous works on linear polyenes and carotenoids as well as a study of the dependence of the results on functional and basis set have revealed that the BLYP/6-31G* combination yields reliable results in comparison with experimental values.[49,50] One can expect that the doubly excited states which are not included in the TDDFT calculations and which are important for neutral carotenoids do not play a relevant role in the radical cations, since the lowest occupied orbital is only singly occupied. All calculations have been performed with the Q-Chem 3.0 program.[51]

Results

Carotenoid Radical Cations in Solution. Four different carotenoids (Vio, lutein (Lut), Zea, and β-carotene (β-Car)) were studied by R2C2PI spectroscopy. The first pump pulse centered at 490 nm excites the carotenoids to the S_2 state, whereas the second pump pulse with a delay time τ_1 has a center wavelength of 775 nm and is resonant with the $S_2 \rightarrow S_N$ transition (Figure 1). Upon carotenoid excitation at 490 nm, the generated S_2 state of all carotenoids exhibits a strong ESA in the near-IR region. Applying the 775 nm pulse while the S_2 state is occupied results in a further excitation of the molecules into the S_N state. The relaxation of this higher excited-state can occur either back to S_2, or a free electron can be released and a carotenoid radical cation is formed. The second pathway is supported by previous studies,[52] and by our experiments, since the second pulse leads to ESA decrease in favor of a new long-lived species attributed in our work to Car$^{\bullet+}$ (see Figure S2). Transient absorption (TA) spectra were measured for different time intervals τ_2 between the first pulse and the probe pulse (Figure 1b).

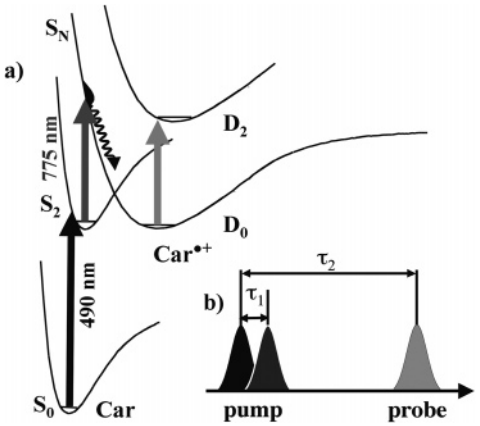

Figure 1. Schematic diagram of the resonant two photon two color ionization (R2C2PI) experiment on carotenoids.

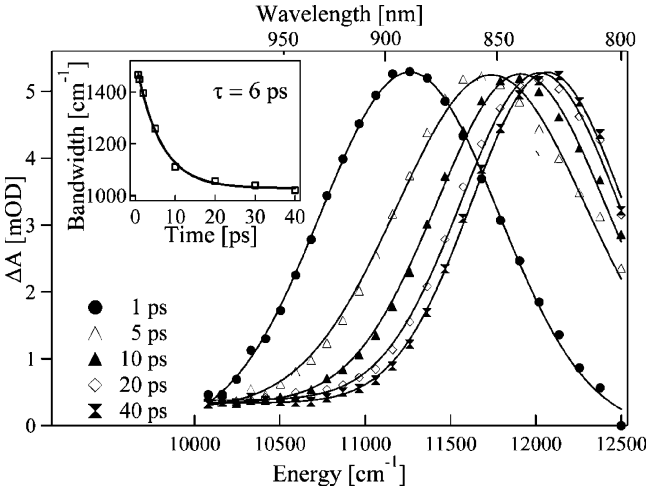

Figure 2. Absorption spectra of $Vio^{\bullet+}$ in ethanol for different time delays (τ_2) after cation generation. The $Vio^{\bullet+}$ bandwidth versus delay time is plotted in the insert.

The TA spectra exhibit a transient signal in the near-IR region from 800 to 1000 nm associated with the $Car^{\bullet+}$ (Figure 2). The spectral amplitude of the cation absorption strongly depends on the time delay between the first two pulses τ_1 (data not shown). The maximum yield of the transient $Car^{\bullet+}$ signal was achieved by tuning the delay time τ_1 to approximately 40 fs. However, the time delay cannot be unambiguously detected since the pulse lengths, which are 100 fs for the first pulse and 250 fs for the second pulse, directly influence the time resolution. When the maximum yield of the $Car^{\bullet+}$ signal was achieved for Vio, τ_1 was kept fixed for all carotenoids, and TA measurements were performed by varying τ_2. The temporal and spectral evolution of the optically generated $Car^{\bullet+}$ species is presented in Figure 2. For simplicity only the Vio data are shown, since the trend is practically identical for all investigated carotenoids.

Upon increasing τ_2 a blue spectral shift concomitant with a narrowing of the $Car^{\bullet+}$ spectrum was observed, indicative of a cooling process in the $Car^{\bullet+}$ ground state. The cooling dynamics was monitored by plotting the bandwidth versus time delay, and an exponential fit results in a time constant of ~6 ps (Figure 2, insert). It should be noted that without the second pulse no transient $Car^{\bullet+}$ signal was detected.

The TA spectra for $\tau_2 = 40$ ps of all four carotenoids studied are shown in Figure 3. At this point, the dynamic evolution of

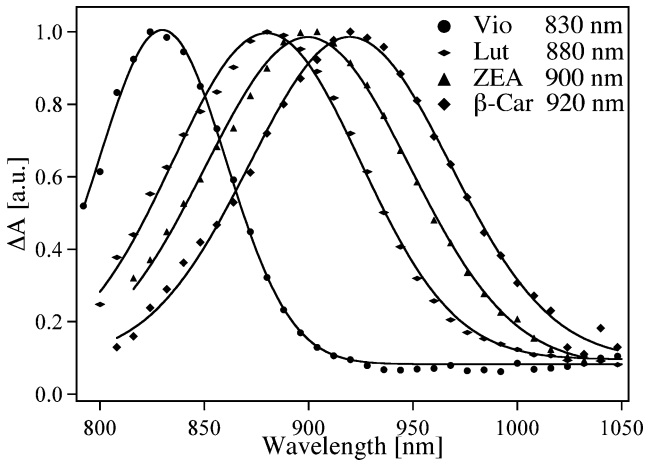

Figure 3. Transient absorption spectra of the investigated $Car^{\bullet+}$ in the near-IR region in ethanol solution, taken 40 ps after generation. From left to right: Vio, Lut, Zea, and β-Car.

TABLE 1: Carotenoid Composition in Native and Zea-Enriched Preparations of LHC II[a]

sample	violaxanthin	neoxanthin	lutein	zeaxanthin
LHC II-Vio	26.6	36	100	0
LHC II-Zea	7.4	35.8	100	12.7

[a] Data are normalized to 100 lutein molecules, represent integration of HPLC peaks measured at 440 nm, and correspond to relative values, though direct comparison between the same carotenoids in the two different samples is possible. Within the experimental accuracy the neoxanthin content of both samples remains unchanged; the violaxanthin content decreases upon the presence of zeaxanthin.

the $Car^{\bullet+}$ spectra was completed, indicating that the cations are in their respective ground states and that the cooling processes are finished.

For ease of comparison, the $Car^{\bullet+}$ spectra are normalized to the same absorbance value at the wavelength of maximum absorption. The $Car^{\bullet+}$ bands have maxima located at 830 nm (Vio), 880 nm (Lut), 900 (Zea), and 920 nm (β-Car). A shift of the $Car^{\bullet+}$ absorption band toward lower energies in the order Vio → Lut → Zea → β-Car according to the increase in conjugation length from Vio (9 C=C) to Lut (10 C=C) to Zea and β-Car (11 C=C) was observed. Surprisingly, although having the same number of C=C double bonds, the excited-state absorption (ESA) observed for β-Car is slightly red-shifted compared to Zea. Comparison of Vio and Zea, the relevant carotenoids for qE, yelds an energy difference of the $D_0 \rightarrow D_2$ transition for $Vio^{\bullet+}$ and $Zea^{\bullet+}$ in ethanol of ~937 cm^{-1} or 0.12 eV.

Chl Excited-State Dynamics in LHC II. Ultrafast PP measurements were performed on native LHC II and on LHC II in which Vio has been biochemically converted to Zea as indicated above. The presence of Zea in LHC II was verified by HPLC analysis. For the LHC II-Vio sample a maximum content of Vio was achieved, and no trace of Zea was detected. In the Zea-enriched LHC II sample (LHC II-Zea) the maximum Zea level exceeds the Vio content almost by a factor of 2 (Table 1). It should be noted that a part of Vio is lost during the conversion.

To study the kinetics of the first excited Chl state in LHC II, the Q_y transition was excited at 660 nm and TA spectra were acquired in the near-IR region from 800 to 1050 nm, where the broad ESA of Chl can be detected. The TA spectra were analyzed using a global fitting routine revealing two major decay components, a fast decay (~10 ps) and a slower decay, with a time constant beyond 1.5 ns, that is, beyond the time scale of

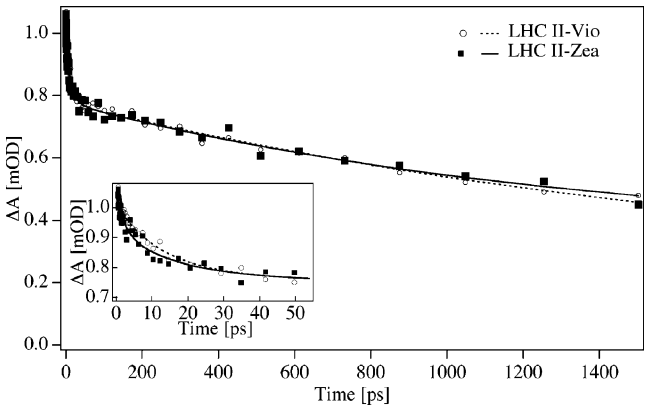

Figure 4. TA data for LHC II-Vio (open circles) and LHC II-Zea (filled squares) detected at 904 nm upon excitation at 660 nm. The solid and dashed lines correspond to the fit curve obtained by a global fitting routine. The TA kinetics is representative for the investigated spectral region from 800 to 1050 nm.

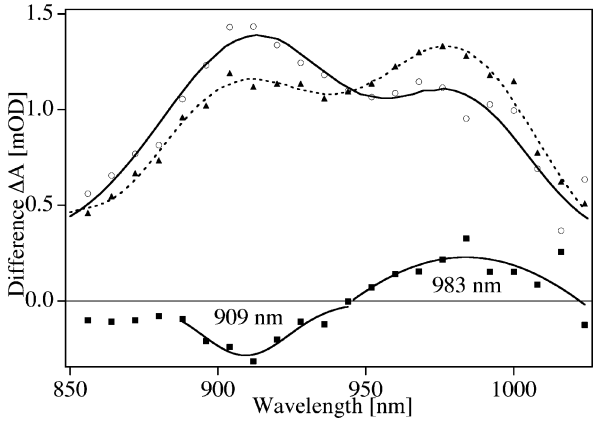

Figure 5. Difference transient absorption spectra between R2C2PI and PP revealing all $Car^{\bullet+}$ in LHC II-Vio (open circles) and LHC II-Zea (filled triangles). The solid and dashed line corresponds to Gaussian fits of the data points. The difference between Zea and Vio LHC II (squares) and the respective Gaussian fits with extremes at 909 and 983 nm reflects the $Vio^{\bullet+}$ and $Zea^{\bullet+}$.

our experiment. The kinetics observed for both LHC II samples, LHC II-Vio and LHC II-Zea, are essentially identical over the entire spectral range investigated, displaying only minor differences, which are not significant within our experimental errors (data not shown). The transient characteristics in the Q_y region are illustrated by the kinetic traces measured at 904 nm (Figure 4). It is important to note that LHC II-Zea samples show no additional rise and decay as reported for thylakoid membranes upon qE induction.[17]

Carotenoid Radical Cation Detection in LHC II. The R2C2PI measurements on carotenoids in solution revealed a transient species identified as $Car^{\bullet+}$ signal in the near-IR region (Figure 3). However, performing R2C2PI measurements on LHC II (Figure 5), leads to a chlorophyll ESA signal as a consequence of EET from S_2 (Car) to Q_y (Chl) which interferes with the detection of $Car^{\bullet+}$. The pump−probe (PP) TA spectra recorded at a delay of 40 ps upon carotenoid excitation into S_2 at 490 nm are dominated by a structureless ESA signal, which originates from excited Chls and cover the entire investigated spectral range. After 40 ps, a large part of the excitation energy is already transferred to Chls as a result of direct EET from the carotenoids. Remaining carotenoid contributions, for instance ESA from S_1, disappear with a time constant around 10 ps as a result of the fast internal conversion (IC) to the ground state.[53] As a consequence, the PP spectrum at 40 ps contains exclusively

TABLE 2: Calculated Maximum Absorption Wavelength λ_{max} (nm) and Excitation Energies of the Most Strongly Allowed $\pi\pi^*$ Excitation of the Carotenoid Radical Cations of Vio, Lut, Zea, and β-Car

	λ_{max} [nm]	ω [eV]	oscillator strength
violaxanthin	753	1.646	2.97
lutein	765	1.620	2.92
zeaxanthin	840	1.476	2.53
β-carotene	845	1.467	2.53

Chl ESA, while a corresponding R2C2PI spectrum contains both Chl ESA and $Car^{\bullet+}$ contributions. The difference between R2C2PI and PP spectrum at 40 ps should thus reflect only the remaining spectral contribution of the thermalized $Car^{\bullet+}$ species. However, also the Chl ESA signal differs in the R2C2PI experiment slightly from the conventional PP experiment, since further excitation of the S_2 state with the second laser pulse results in a loss of potential carotenoid donors for the EET toward the Chls, and consequently the Chl ESA signal will decrease. On the other hand, hot S_2 states may be produced in the R2C2PI experiment, which can have an increased Car → Chl transfer rate. In any case these phenomena only result in a shift of the baseline and do not disturb the analysis.

The transient difference spectra at 40 ps time delay obtained by this procedure for the LHC II-Vio and LHC II-Zea samples are presented in Figure 5. This is a sum of all carotenoid radical cations spectroscopically generated in LHC II (Table 1). A Gaussian fit of the difference TA spectrum Zea−Vio results in a negative contribution at 909 nm and a positive one at 983 nm. The energy gap between them is 828 cm^{-1} or 0.10 eV, close to the energy gap of 0.12 eV between $Vio^{\bullet+}$ and $Zea^{\bullet+}$ found for Vio and Zea in solution. Recent voltammetric oxidation studies,[54] reveal the energy difference between the oxidation potential of Vio and Zea (0.29 eV). Since we probe the D_0—D_2 transition, a direct comparison between electrochemical data and our values is only valid, for the unlikely assumption that the S_0—D_2 energy difference is unchanged for Vio and Zea. A deviation of ΔE (S_0—D_2) may explain the observed difference.

In comparison with the solution spectra, the absorption maxima of $Car^{\bullet+}$ in LHC II are generally red-shifted by about 80 nm.

Quantum Chemical Calculations of Carotenoid Radical Cations. As a first step, the geometries of the carotenoid radical cations were optimized starting from the energetically lowest conformers of the corresponding neutral carotenoids.[49,55] All carotenoid cations exhibit an open-shell doublet ground state. At the obtained equilibrium geometries, the 10 lowest vertical excited states of the radical cations of Vio, Lut, Zea, and β-Car have been calculated and analyzed in detail. In this context, only the strongly allowed $\pi\pi^*$ transition observed in the fs experiments is of interest. At the theoretical level of TDDFT/BLYP/6-31G* the cations of Vio, Lut, Zea, and β-Car exhibit strongly allowed transitions with excitation wavelengths of 753, 765, 840, and 845 nm, respectively (Table 2), in agreement with the experimental energetic ordering. These states correspond to $\pi\pi^*$ transitions, whose main contributions are the transitions of the unpaired electron from the highest occupied molecular orbital to the lowest unoccupied one. As an example, these orbitals are displayed for $Vio^{\bullet+}$ in Figure 6, which are essentially the same molecular orbitals like the ones relevant for the optically allowed S_2 states of the neutral species.

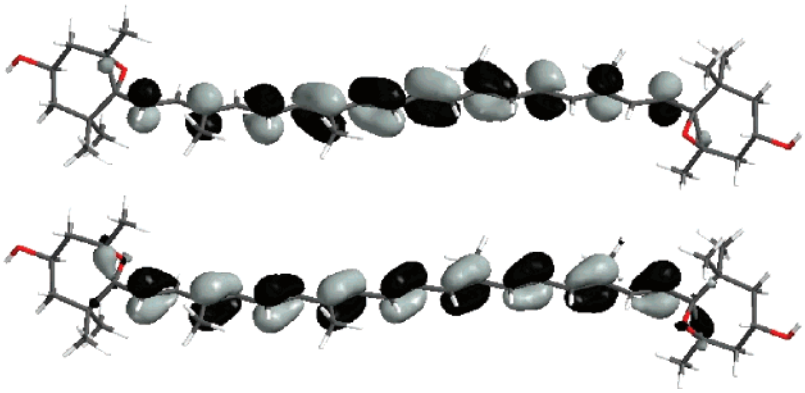

Figure 6. Highest occupied (bottom) and lowest unoccupied (top) molecular orbital of the violaxanthin radical cation.

Discussion

Carotenoid Radical Cation in Solution. In the R2C2PI experiments a long-lived species with a TA signal in the near-IR region was observed for all four investigated carotenoids in ethanol. In previous experiments, transient $Car^{\bullet+}$ species were created by ionization, which vanish only after charge recombination, a process which occurs typically within ps to μs.[56] Previously reported pump−deplete−probe (PDP) experiments on lycopene showed a persistent loss of excited-state population after re-excitation of the S_2 ESA at 795 nm.[57] No product state was observed, and the repumped population disappeared, most probably deposited in a long-lived $Car^{\bullet+}$ state with no clear spectral signature in the probed region. Similarly, double-pump techniques have been applied to peridinin, where an 800-nm pulse was applied soon after carotenoid excitation. Thereby, a part of the S_2 population was transferred to a higher excited-state obtaining a photoproduct state persisting on a nanosecond time scale, and attributed to peridinin cations on the basis of their $D_0 \rightarrow D_2$ transition detected in the near-IR region.[52] Our R2C2PI experiments performed on carotenoids solubilized in ethanol show a similar transient species, which can unambiguously be assigned to $Car^{\bullet+}$, in agreement with previous measurements.

The evolution of the transient absorption bands of the $Car^{\bullet+}$ between 1 and 40 ps (Figure 2) is in all cases dominated by a substantial narrowing of the ESA band and by a significant blue shift (e.g., from 885 to 830 nm for Vio in ethanol) of the absorption maximum. This is typical for cooling processes which are due to energy transfer from the $Car^{\bullet+}$ to the solvent (vibrational cooling).

As illustrated by our measurements of the various $Car^{\bullet+}$ species in ethanol (Figure 3) and the quantum chemical calculations (Table 2), the order of the excitation energies of the lowest strongly absorbing states in the near-IR region is Vio > Lut > Zea > β-Car. The decrease in excitation energies from Vio to Lut and Zea goes parallel with the increasing number of conjugated double bonds in agreement with a simple particle-in-a-box model. It is, however, astonishing that compared to $Zea^{\bullet+}$, β-$Car^{\bullet+}$ is red-shifted by 20 nm in ethanol and 5 nm in the quantum chemical calculations, respectively, since both contain eleven conjugated double bonds. The small energetic difference in the calculation disregarding any solvent effects can probably be attributed to the additional OH groups in Zea, which are the only major chemical difference, whereas all other geometrical parameters are essentially the same in the two compounds. In ethanol, the difference in the excitation energies is a factor of 4 larger than the quantum chemical calculation values, which could be due to a better stabilization of the excited-state of Zea compared to the one of β-Car. In contrast to β-Car, Zea can form hydrogen bonds with ethanol via the additional OH groups, and the polar solvent may interact favorably with the local dipoles of the Zea hydroxyl groups. Preliminary calculations of the excited states of Zea bound to one ethanol molecule via a hydrogen bond indicate that the excited-state increases in energy from 1.476 eV (840 nm) to 1.493 eV (829 nm). Similar explicit solvent effects can be expected to be responsible for the different shifts in the quantum chemical calculations and the experimental values obtained in ethanol when the other carotenoids are compared.

In general, $Car^{\bullet+}$ absorption strongly depends on the solvent as previous β-Car studies illustrate. For example, β-Car absorbs at 935 nm in acetonitrile,[37] and 970 nm in dichloromethane.[58] However, since the overall structure of the carotenoids is very similar, one can expect differences due to implicit solvent effects to be quite similar for different species, while direct interactions like H-bond formation are more important to explain small differences between similar carotenoids. In summary, the general position of the absorption band is determined by the polarizability of the solvent and the number of conjugated double bonds of the carotenoid, while small differences in the absorption spectra of similar carotenoids of the same length are due to subtle differences in the molecular structure of different carotenoids as has been pointed out for Zea and β-Car.

Dynamics of the First Excited Chl State in LHC II. The analysis of our TA measurements on LHC II-Vio and LHC II-Zea samples upon Q_y excitation revealed two kinetic components, a fast 10 ps and a slow >1.5 ns component necessary to describe the ESA dynamics at a probe wavelength of 904 nm (Figure 4). Earlier time-resolved PP measurements of trimeric LHC II have revealed EET from Chl *b* → Chl *a* which occurs with kinetic components of ~150 fs, 600 fs at room temperature and at 77 K,[59−62] and equilibration among the Chl *a* molecules taking place with time constants longer than 10 ps.[61−63] In agreement with these earlier measurements we assign the fast 10 ps component to equilibration processes between Chl *a* molecules. The slow decay >1.5 ns can be attributed to the excited-state lifetime of Chl *a* molecules.

Several models for the qE component of NPQ have been proposed and are still discussed controversially. A recent model for qE suggests that the replacement of Vio by Zea in its LHC II binding pocket can in principle result in qE via the so-called "gear-shift" mechanism. The latter requires the Vio S_1 state to be higher in energy than the Q_y of Chl *a*, and the S_1 state of Zea to be lower. However, recent experiments on Vio and Zea solubilized in organic solvents and bound to recombinant LHC II have shown that the S_1 energies exhibit no major difference and lie below the excited-state of Chl *a*:[53,64,65] According to TA measurements, the S_1 energies of Vio and

Zea exhibit values of 1.79 and 1.74 eV in solution and 1.70 and 1.71 eV in recombinant LHC-II, while fluorescence measurements give 1.84 and 1.80 eV. The difference in the values obtained from TA and fluorescence is consistently explained by geometry relaxation effects.[49] In summary, it is unclear whether the quenching of Chl excited states can occur via EET to the Zea S_1 state or via another mechanism, such as ET.

However, it should be noted that the addition of excess Zea to LHC II in detergent solution has been reported to induce fluorescence quenching.[66] On the other hand, Mullineaux et al. show that the Zea/Vio ratio in LHC II has no influence on the time-resolved fluorescence emission spectrum.[67] The authors report a decrease of the fluorescence lifetime from 4.3 ns in the solubilized LHC II to 110 ps in a semicrystalline aggregated state. They also state that the quenching species is a nonfluorescent pigment, which cannot be resolved by time-resolved fluorescence measurements. This difficulty is overcome by our measurements since here we measure ESA and can thus detect also nonfluorescent (dark) states.

In our experiments, upon Q_y excitation of Chls, no additional rise and decay attributed to $Car^{\bullet+}$ during qE was detected throughout the entire investigated spectral range (800−1050 nm). Furthermore, the replacement of Vio to Zea in the LHC II binding site of Vio has no effect on Chl excitation lifetime (Figure 4), and no evidence of chlorophyll fluorescence quenching has been found. Since the chlorophyll fluorescence lifetime is typically 2.5 ns it is unlikely that relevant changes occur beyond our experimentally covered time range of 1.5 ns. In any case, it can be concluded that a significant Chl quenching leading to a reduced lifetime of typically 0.2 ns for qE does not occur. Thus, the simple quenching model mentioned above, according to which LHC II as the site of qE,[34] has to be revised, and other factors have to be taken into account. For example, if PsbS is indeed necessary for maximum qE, its absence in our preparations may explain why quenching did not occur.

Carotenoid Radical Cation Detection in LHC II. One goal of the present work was to investigate and characterize possible carotenoid cations in LHC II and to understand their role in qE. Figure 5 presents the R2C2PI−PP difference spectra of LHC II-Vio and LHC II-Zea samples which correspond to sums of all different carotenoid cations spectroscopically generated in the R2C2PI experiment (Vio, Neo, Lut, Zea). For the analysis of Figure 5, variable contributions of the different carotenoids are anticipated according to their relative amount generated in the corresponding samples. The cation signal of Lut can thus be expected to be approximately three times larger than that of Vio in the LHC II-Vio sample (see pigment analysis in Table 1). On the other hand, the transiently populated S_2 states of the different carotenoids interact differently with the second pulse. For example, the S_2 population of Vio may have a larger spectral overlap with the second pulse, since its $S_2 \rightarrow S_N$ band is blue-shifted compared to that of Lut. Thus, assuming that the first pulse excites approximately the same amount of carotenoids, the amount of cation generation is ultimately dependent on the second pulse. As a result, the correlation between the amount of neutral carotenoids and the amount of cations generated by means of R2P2CI is lost. Nevertheless, all these phenomena have influence only on the amplitude of the cation band and not on λ_{max}. Therefore, subtraction of LHC II Vio cations generated by R2C2PI from LHC II Zea results in a cancellation of Neo and Lut cation contributions whose amounts are identical in Vio and Zea LHC II samples, and only a negative and a positive signal remains corresponding to the decrease of Vio and the increase of Zea cations.

Because of the difference in the amount of Zea and Vio bound to those samples, and the differences observed also in our TA measurements, we are able to attribute the transient spectral maximum at 909 nm to $Vio^{\bullet+}$ and at 983 nm to $Zea^{\bullet+}$. In LHC II the absorption bands of the cations are shifted to lower energies compared to ethanol which is a result of interactions with the protein environment in LHC II. The observed shift of the carotenoid radical absorption band in LHC II toward lower energies from Vio to Zea is similar to their shift in solution and to corresponding quantum chemical calculations. This is also in agreement with earlier measurements on photosystem II core complex mutants from *Synechocystis* sp. PCC 6803, where upon replacement of the natural β-carotene (11 C═C) by β-zeacarotene (β-Zea) (9 C═C), a blue shift for the corresponding carotenoid cations from 984 nm (β-$Car^{\bullet+}$) to 898 nm (β-$Zea^{\bullet+}$), has been observed.[64]

The energy difference between the allowed excited states in the near-IR of $Vio^{\bullet+}$ and $Zea^{\bullet+}$ is ∼1370 cm^{-1} or 0.17 eV according to our quantum chemical calculations, but only ∼937 cm^{-1} or 0.12 eV according to our solution measurements, and in LHC II it is only 828 cm^{-1} or 0.10 eV. Obviously, as already pointed out for the solution studies, also the LHC II protein environment has different effects on different carotenoids.[34] Zea has a similar overall molecular structure as Vio, except that it lacks the epoxy groups at either end and that the terminal β-ionone rings are less twisted.

Our measurements on the LHC II samples do not directly reveal the position of $Lut^{\bullet+}$ absorption, but according to the energetic order from the solution measurements and taking into account the red shift caused by protein binding, one can estimate the location of the $Lut^{\bullet+}$ absorption to be at ∼960 nm, and the one of β-$Car^{\bullet+}$ to be around 1000 nm. Previous studies on spinach photosystem II membranes found the β-$Car^{\bullet+}$ λ_{max} at 996 nm.[36]

Location and Mechanism of qE. Our TA measurements on LHC II-Vio and LHC II-Zea samples indicate that simple replacement of Vio by Zea in LHC II is not sufficient for chlorophyll fluorescence quenching. Furthermore, we found in our R2C2PI measurements the position of the Zea cation in LHC_II at 983 nm, which is about 20 nm blue-shifted compared to the carotenoid cation which was previously identified during qE.[17] Today it is well-established that Zea, and to a smaller extent, Lut, affect the rate of qE induction and the net amount of quenching.[68] Steady-state absorption experiments on leaves and intact thylakoid membranes indicate that Zea undergoes spectroscopic changes during qE, that is, a rise of the 535 nm band in the difference spectrum was ascribed to a red shift of the Zea.[28]

As pointed out in the introduction, it is proposed that upon qE induction the PsbS monomers associated with the LHC antenna are responsible for in vivo energy dissipation.[29−31] Thus, if Zea indeed binds to the same site as Vio in LHC II, one Zea OH group would be buried, but the other one would be accessible from the hydrophobic membrane environment. If one still wants to retain the model which proposes Zea bound to LHC II as the quenching site, one possible candidate to complete this model is PsbS, which may provide a highly polar environment that strongly affects the photophysical properties of Zea during qE induction. As a result, Chl excitation energy can be quenched.

As a next step, we plan to perform R2C2PI experiments on LHC II in the presence of PsbS to study whether a LHC II/

PsbS complex leads to a $Zea^{\bullet+}$ signal at the same wavelength (1000 nm) as the one found during qE. This might confirm our proposed qE mechanism and would finally identify the location of qE in the photosynthetic apparatus of green plants.

Acknowledgment. This work has been supported by the SFB 472 ("Molecular Bioenergetics"), as well as by the "Center for Membrane Proteomics" of the University of Frankfurt. A.D. is supported by the Deutsche Forschungsgemeinschaft as an "Emmy Noether" fellow, and T.B. by the fellowship SFRH/BD/21440/2005 from Fundação para a Ciência e Tecnologia.

Supporting Information Available: Transient absorption spectra and kinetics. This material is available free of charge via the Internet at http://pubs.acs.org.

References and Notes

(1) Polivka, T.; Sundstrom, V. *Chem. Rev.* **2004**, *104*, 2021.
(2) Frank, H. A.; Cogdell, R. J. *Photochem. Photobiol.* **1996**, *63*, 257.
(3) Peter, G. F.; Thornber, J. P. *J. Biol. Chem.* **1991**, *266*, 16745.
(4) Jansson, S. *Biochim. Biophys. Acta Bioenerg.* **1994**, *1184*, 1.
(5) Foote, C. S. *Science* **1968**, *162*, 963.
(6) Foote, C. S.; Chang, Y. C.; Denny, R. W. *J. Am. Chem. Soc.* **1970**, *92*, 5216.
(7) Renger, G.; Wolff, C. *Biochim. Biophys. Acta* **1977**, *460*, 47.
(8) Niyogi, K. K. *Annu. Rev. Plant Physiol. Plant Mol. Biol.* **1999**, *50*, 333.
(9) Griffiths, M.; Sistrom, W. R.; Cohenbazire, G.; Stanier, R. Y. *Nature* **1955**, *176*, 1211.
(10) Frank, H. A. *The Photochemistry of Carotenoids*; Kluwer: Dordrecht, The Netherlands, 1999; Vol. 8.
(11) Muller, P.; Li, X. P.; Niyogi, K. K. *Plant Physiol.* **2001**, *125*, 1558.
(12) Horton, P.; Ruban, A. V.; Walters, R. G. *Annu. Rev. Plant Physiol. Plant Mol. Biol.* **1996**, *47*, 655.
(13) Li, X. P.; Bjorkman, O.; Shih, C.; Grossman, A. R.; Rosenquist, M.; Jansson, S.; Niyogi, K. K. *Nature* **2000**, *403*, 391.
(14) Li, X. P.; Gilmore, A. M.; Caffarri, S.; Bassi, R.; Golan, T.; Kramer, D.; Niyogi, K. K. *J. Biol. Chem.* **2004**, *279*, 22866.
(15) Frank, H. A.; Cua, A.; Chynwat, V.; Young, A.; Gosztola, D.; Wasielewski, M. R. *Photosynth. Res.* **1994**, *41*, 389.
(16) Pascal, A. A.; Liu, Z. F.; Broess, K.; van Oort, B.; van Amerongen, H.; Wang, C.; Horton, P.; Robert, B.; Chang, W. R.; Ruban, A. *Nature* **2005**, *436*, 134.
(17) Holt, N. E.; Zigmantas, D.; Valkunas, L.; Li, X. P.; Niyogi, K. K.; Fleming, G. R. *Science* **2005**, *307*, 433.
(18) Demmigadams, B. *Biochim. Biophys. Acta* **1990**, *1020*, 1.
(19) Berera, R.; Herrero, C.; van Stokkum, L. H. M.; Vengris, M.; Kodis, G.; Palacios, R. E.; van Amerongen, H.; van Grondelle, R.; Gust, D.; Moore, T. A.; Moore, A. L.; Kennis, J. T. M. *Proc. Natl. Acad. Sci. U.S.A.* **2006**, *103*, 5343.
(20) Horton, P.; Ruban, A. V.; Rees, D.; Pascal, A. A.; Noctor, G.; Young, A. J. *FEBS Lett.* **1991**, *292*, 1.
(21) Dreuw, A.; Fleming, G. R.; Head-Gordon, M. *J. Phys. Chem. B* **2003**, *107*, 6500.
(22) Dreuw, A.; Fleming, G. R.; Head-Gordon, M. *Phys. Chem. Chem. Phys.* **2003**, *5*, 3247.
(23) Dreuw, A.; Fleming, G. R.; Head-Gordon, M. *Biochem. Soc. Trans.* **2005**, *33*, 858.
(24) Gilmore, A. M.; Hazlett, T. L.; Govindjee. *Proc. Natl. Acad. Sci. U.S.A.* **1995**, *92*, 2273.
(25) Aspinall-O'Dea, M.; Wentworth, M.; Pascal, A.; Robert, B.; Ruban, A.; Horton, P. *Proc. Natl. Acad. Sci. U.S.A.* **2002**, *99*, 16331.
(26) Ruban, A. V.; Young, A. J.; Horton, P. *Plant Physiol.* **1993**, *102*, 741.
(27) Bilger, W.; Bjorkman, O. *Planta* **1994**, *193*, 238.
(28) Ruban, A. V.; Pascal, A. A.; Robert, B.; Horton, P. *J. Biol. Chem.* **2002**, *277*, 7785.
(29) Bergantino, E.; Segalla, A.; Brunetta, A.; Teardo, E.; Rigoni, F.; Giacometti, G. M.; Szabo, I. *Proc. Natl. Acad. Sci. U.S.A.* **2003**, *100*, 15265.
(30) Li, X. P.; Phippard, A.; Pasari, J.; Niyogi, K. K. *Funct. Plant Biol.* **2002**, *29*, 1131.
(31) Jansson, S. *Trends Plant Sci.* **1999**, *4*, 236.
(32) Holt, N. E.; Fleming, G. R.; Niyogi, K. K. *Biochemistry* **2004**, *43*, 8281.
(33) Liu, Z. F.; Yan, H. C.; Wang, K. B.; Kuang, T. Y.; Zhang, J. P.; Gui, L. L.; An, X. M.; Chang, W. R. *Nature* **2004**, *428*, 287.
(34) Standfuss, J.; Terwisscha van Scheltinga, A. C.; Lamborghini, M.; Kuhlbrandt, W. *EMBO J.* **2005**, *24*, 919.
(35) Schenck, C. C.; Diner, B.; Mathis, P.; Satoh, K. *Biochim. Biophys. Acta* **1982**, *680*, 216.
(36) Tracewell, C. A.; Brudvig, G. W. *Biochemistry* **2003**, *42*, 9127.
(37) Polyakov, N. E.; Leshina, T. V.; Salakhutdinov, N. F.; Kispert, L. D. *J. Phys. Chem. B* **2006**, *110*, 6991.
(38) Polivka, T.; Pullerits, T.; Frank, H. A.; Cogdell, R. J.; Sundstrom, V. *J. Phys. Chem. B* **2004**, *108*, 15398.
(39) Polivka, T.; Zigmantas, D.; Herek, J. L.; He, Z.; Pascher, T.; Pullerits, T.; Cogdell, R. J.; Frank, H. A.; Sundstrom, V. *J. Phys. Chem. B* **2002**, *106*, 11016.
(40) Muller-Moule, P.; Conklin, P. L.; Niyogi, K. K. *Plant Physiol.* **2002**, *128*, 970.
(41) Burke, J. J.; Ditto, C. L.; Arntzen, C. J. *Arch. Biochem. Biophys.* **1978**, *187*, 252.
(42) Gilmore, A. M.; Yamamoto, H. Y. *J. Chromatogr.* **1991**, *543*, 137.
(43) Huber, R.; Satzger, H.; Zinth, W.; Wachtveitl, J. *Opt. Commun.* **2001**, *194*, 443.
(44) Lenz, M. O.; Huber, R.; Schmidt, B.; Gilch, P.; Kalmbach, R.; Engelhard, M.; Wachtveitl, J. *Biophys. J.* **2006**, *91*, 255.
(45) Becke, A. D. *J. Chem. Phys.* **1993**, *98*, 5648.
(46) Dreuw, A.; Head-Gordon, M. *Chem. Rev.* **2005**, *105*, 4009.
(47) Runge, E.; Gross, E. K. U. *Phys. Rev. Lett.* **1984**, *52*, 997.
(48) Becke, A. D. *Phys. Rev. A: At., Mol., Opt. Phys.* **1988**, *38*, 3098.
(49) Dreuw, A. *J. Phys. Chem. A* **2006**, *110*, 4592.
(50) Hsu, C. P.; Hirata, S.; Head-Gordon, M. *J. Phys. Chem. A* **2001**, *105*, 451.
(51) Shao, Y.; Molnar, L. F.; Jung, Y.; Kussmann, J.; Ochsenfeld, C.; Brown, S. T.; Gilbert, A. T. B.; Slipchenko, L. V.; Levchenko, S. V.; O'Neill, D. P.; DiStasio, R. A.; Lochan, R. C.; Wang, T.; Beran, G. J. O.; Besley, N. A.; Herbert, J. M.; Lin, C. Y.; Van Voorhis, T.; Chien, S. H.; Sodt, A.; Steele, R. P.; Rassolov, V. A.; Maslen, P. E.; Korambath, P. P.; Adamson, R. D.; Austin, B.; Baker, J.; Byrd, E. F. C.; Dachsel, H.; Doerksen, R. J.; Dreuw, A.; Dunietz, B. D.; Dutoi, A. D.; Furlani, T. R.; Gwaltney, S. R.; Heyden, A.; Hirata, S.; Hsu, C. P.; Kedziora, G.; Khalliulin, R. Z.; Klunzinger, P.; Lee, A. M.; Lee, M. S.; Liang, W.; Lotan, I.; Nair, N.; Peters, B.; Proynov, E. I.; Pieniazek, P. A.; Rhee, Y. M.; Ritchie, J.; Rosta, E.; Sherrill, C. D.; Simmonett, A. C.; Subotnik, J. E.; Woodcock, H. L.; Zhang, W.; Bell, A. T.; Chakraborty, A. K.; Chipman, D. M.; Keil, F. J.; Warshel, A.; Hehre, W. J.; Schaefer, H. F.; Kong, J.; Krylov, A. I.; Gill, P. M. W.; Head-Gordon, M. *Phys. Chem. Chem. Phys.* **2006**, *8*, 3172.
(52) Papagiannakis, E.; Vengris, M.; Larsen, D. S.; van Stokkum, I. H. M.; Hiller, R. G.; van Grondelle, R. *J. Phys. Chem. B* **2006**, *110*, 512.
(53) Polivka, T.; Zigmantas, D.; Sundstrom, V.; Formaggio, E.; Cinque, G.; Bassi, R. *Biochemistry* **2002**, *41*, 439.
(54) Niedzwiedzki, D.; Rusling, J. F.; Frank, H. A. *Chem. Phys. Lett.* **2005**, *416*, 308.
(55) Schlucker, S.; Szeghalmi, A.; Schmitt, M.; Popp, J.; Kiefer, W. *J. Raman Spectrosc.* **2003**, *34*, 413.
(56) Pan, J.; Benko, G.; Xu, Y. H.; Pascher, T.; Sun, L. C.; Sundstrom, V.; Polivka, T. *J. Am. Chem. Soc.* **2002**, *124*, 13949.
(57) Wohlleben, W.; Buckup, T.; Herek, J. L.; Motzkus, M. *ChemPhysChem* **2005**, *6*, 850.
(58) Jeevarajan, J. A.; Wei, C. C.; Jeevarajan, A. S.; Kispert, L. D. *J. Phys. Chem.* **1996**, *100*, 5637.
(59) Savikhin, S.; Vanamerongen, H.; Kwa, S. L. S.; Vangrondelle, R.; Struve, W. R. *Biophys. J.* **1994**, *66*, 1597.
(60) Bittner, T.; Irrgang, K. D.; Renger, G.; Wasielewski, M. R. *J. Phys. Chem.* **1994**, *98*, 11821.
(61) Palsson, L. O.; Spangfort, M. D.; Gulbinas, V.; Gillbro, T. *FEBS Lett.* **1994**, *339*, 134.
(62) Kleima, F. J.; Gradinaru, C. C.; Calkoen, F.; vanStokkum, I. H. M.; vanGrondelle, R.; vanAmerongen, H. *Biochemistry* **1997**, *36*, 15262.
(63) Linnanto, J.; Martiskainen, J.; Lehtovuori, V.; Ihalainen, J.; Kananavicius, R.; Barbato, R.; Korppi-Tommola, J. *Photosynth. Res.* **2006**, *87*, 267.
(64) Frank, H. A.; Bautista, J. A.; Josue, J. S.; Young, A. J. *Biochemistry* **2000**, *39*, 2831.
(65) Polivka, T.; Herek, J. L.; Zigmantas, D.; Akerlund, H. E.; Sundstrom, V. *Proc. Natl. Acad. Sci. U.S.A.* **1999**, *96*, 4914.
(66) Wentworth, M.; Ruban, A. V.; Horton, P. *FEBS Lett.* **2000**, *471*, 71.
(67) Mullineaux, C. W.; Pascal, A. A.; Horton, P.; Holzwarth, A. R. *Biochim. Biophys. Acta* **1993**, *1141*, 23.
(68) Crouchman, S.; Ruban, A.; Horton, P. *FEBS Lett.* **2006**, *580*, 2053.